DEVCOM DAC-TR-2021-091
November 2021

Expanded Methodology of Combined Spinal HIPC/IARC Development for WIAMan

by Cameron R. Bass, Maria Ortiz-Paparoni, David R. Barnes, and Kathryn L. Loftis

DISCLAIMER

The findings in this report are not to be construed as an official Department of the Army position unless so specified by other official documentation.

WARNING

Information and data contained in this document are based on the input available at the time of preparation.

TRADE NAMES

The use of trade names in this report does not constitute an official endorsement or approval of the use of such commercial hardware or software. The report may not be cited for purposes of advertisement.

DEVCOM DAC-TR-2021-091
November 2021

Expanded Methodology of Combined Spinal HIPC/IARC Development for WIAMan

by Cameron R. Bass and Maria Ortiz-Paparoni
Duke University

David R. Barnes
SURVICE Engineering

Kathryn L. Loftis
DEVCOM Data & Analysis Center

REPORT DOCUMENTATION PAGE

Form Approved
OMB No. 0704-0188

1. REPORT DATE	2. REPORT TYPE	3. DATES COVERED (From - To)
November 2021	Technical Report	1/15/2021–8/19/2021

4. TITLE AND SUBTITLE
Expanded Methodology of Combined Spinal HIPC/IARC Development for WIAMan

5a. CONTRACT NUMBER

5b. GRANT NUMBER

5c. PROGRAM ELEMENT NUMBER

6. AUTHOR(S)
Cameron R. Bass, Maria Ortiz-Paparoni, David R. Barnes, and Kathryn L. Loftis

5d. PROJECT NUMBER

5e. TASK NUMBER

5f. WORK UNIT NUMBER

7. PERFORMING ORGANIZATION NAME(S) AND ADDRESS(ES)
Director
DEVCOM Data & Analysis Center
6896 Mauchly Street
Aberdeen Proving Ground, MD

8. PERFORMING ORGANIZATION REPORT NUMBER

DEVCOM DAC-TR-2021-091

9. SPONSORING / MONITORING AGENCY NAME(S) AND ADDRESS(ES)

10. SPONSOR/MONITOR'S ACRONYM(S)

11. SPONSOR/MONITOR'S REPORT NUMBER(S)

12. DISTRIBUTION / AVAILABILITY STATEMENT
DISTRIBUTION STATEMENT A. Approved for public release: distribution unlimited.

13. SUPPLEMENTARY NOTES

14. ABSTRACT
Traditional translational methods used to develop an anthropometric test device (ATD) injury assessment reference curve (IARC) from a human injury probability curve (HIPC), such as match-paired testing or perfect biofidelity, rely on the capability of the ATD to mimic the human behavior under the corresponding loading and boundary conditions. However, the degree of biofidelity is limited by constraints and design requirements; and matched pair testing can result in an overestimation of the injury point due to intrinsic differences in both material behavior and performance to failure between the ATD and human. Injuries at large occur under an initial condition that results in an energy input. To ensure that the testing conditions between a postmortem human subject (PMHS) and ATD are comparable, this study proposes an energy equivalency method to translate the human injury response to an ATD injury assessment reference value (IARV) or an IARC. A human injury probability curve for single or multiple vertebral fracture of the lumbar spine under combined loading was derived from 75 cadaveric tests. The HIPC was then used to inform the generation of an IARC for the WIAMan ATD through energy equivalency methods. To translate the PMHS HIPC data to the ATD IARC, the aggregated PMHS and ATD force-energy responses were generated to determine the transfer function from PMHS measurement to ATD measurements at isoenergy.

15. SUBJECT TERMS
isoenergy translation, Injury Assessment Reference Values (IARVs), Injury Assessment Reference Curves (IARCs), Human Injury Probability Curve (HIPC), dynamic combined loading, lumbar spine, anthropometric test device (ATD)

16. SECURITY CLASSIFICATION OF:			17. LIMITATION OF ABSTRACT	18. NUMBER OF PAGES	19a. NAME OF RESPONSIBLE PERSON
a. REPORT	b. ABSTRACT	c. THIS PAGE			Kathryn Loftis
UNCLASSIFIED	UNCLASSIFIED	UNCLASSIFIED	UU	32	19b. TELEPHONE NUMBER (include area code) 410-306-0344

Table of Contents

List of Figures

1. INTRODUCTION

Injury assessment reference values (IARVs) and injury assessment reference curves (IARCs) have been widely used in multiple applications, such as the enhancement and development of occupant restraint systems, anthropometric test devices (ATDs), airbag systems, policy regulation, and retrospective analysis of injuries in the field, among others.[1–7] In particular, studies have directly defined human injury tolerance values from cadaveric, animal, volunteer, and real-world injury rates to inform ATD performance requirements.[5,8–11] To develop IARCs, a widely used approach is the traditional match-paired testing, where both the ATD and postmortem human subject (PMHS) are evaluated under similar loading, boundary, and initial test conditions, often with energy-based input such as velocity inputs.[12] While this method allows the development of a direct correlation of measured ATD responses to PMHS injury outcomes, there are two areas that limit the effectiveness of this approach in developing IARCs. First, there are potential differences in stiffness between the ATD and cadaveric or animal surrogates. Second, the ATD is intended to remain intact under potentially injurious loading where the cadaver or animal may suffer fractures or failures that compromise the load-bearing capacity. This effect limits peak forces and moments that may be developed in the cadavers or animals compared with the "matched" ATD tests. This limitation of matched pair testing will cause an overestimation of the injury risk estimates in ATDs compared with cadavers, resulting in higher, less conservative injury values.

In general, injuries in humans, animals, or cadavers occur under an initial velocity or impulse condition that results in an energy input. Using an energy equivalency method for the IARC generation ensures that there are comparable testing conditions for the PMHS and ATD despite the stiffness differences across the two components.

In this study, a human injury probability curve (HIPC) for single or multiple vertebral fracture of the lumbar spine was derived from 75 cadaveric tests. In contrast with previously presented curves,[13] the proposed HIPC incorporates a combined loading metric to account for the influences of both the axial force and the bending moment on the injury outcome. The HIPC was then used to inform the generation of an IARC for the WIAMan ATD through energy equivalency methods. To translate the PMHS HIPC data to the ATD IARC, the aggregated PMHS and ATD force-energy responses were generated to determine the transfer function from PMHS measurement to ATD measurements at isoenergy. In the following section, the combined lumbar injury risk IARC (LS-05) will be used as an example of this approach.

2. LUMBAR SPINE VERTEBRAL BODY FRACTURE HIPC

2.1. Moment Decorrelation

To provide a consistent basis for comparison across tests, collected load cell data may be translated to some anatomical reference locations via rigid body transformations. While the forces at T12/L1 are equal to those of the sensing element of the load cell, the moment translation is directly correlated to the axial force (Equation 1).

$$My_{T12/L1} = My_{Load\ Cell} + Fz_{Load\ Cell} * x + Fx_{Load\ Cell} * z \quad (1)$$

where F_z is the compressive axial force, F_x is the anterioposterior sagittal force, x is the anterioposterior distance of the sensing element of the load cell to the estimated geometrical center of the T12/L1 IVD, and z is the superior-inferior distance of the sensing element of the load cell to the T12/L1 IVD center.

When experiments are predominantly compression dominated (such as in the recent combined lumbar risk assessment for WIAMan – LS05) such that F_x is a small fraction of the overall compressive force (i.e., generally less than 5%–10% of the compressive force), there is a strong correlation of the translated moment to the axial force and anterioposterior translation (moment arm) (Figure 1). Small variances in the estimation of the moment arm may result in large variations of the bending moment, introducing moment values associated to the poor estimation of the bending moment about the joint rather than the actual moment applied to the joint. To minimize these effects and have a better representation of the true moment on the T12/L1 joint and to avoid “double counting” of the moment contribution to injury risk assessments, we determine the moment arm by minimizing the correlation between axial force and bending moment.

For combined loading injury criteria, the use of the effective moment center at T12-L1 allows us to avoid spurious bending moments that are correlated with F_z but do not provide additional stress from bending on the anterior or posterior surface of the functional spinal unit. Errors in assessing the actual biomechanical moment center increase the correlation between the axial force (F_z) component and the bending moment (M_y) component, adding uncertainty to the determination of a combined injury criteria. To reduce this uncertainty and account for the independent effects of M_y and F_z in the lumbar injury criteria (L_{ic}), the moment arm of the bending moment was optimized to minimize the correlation between the bending moment (M_y) and the axial force (F_z) at T12 during the loading phase of an experiment (Figure 2).

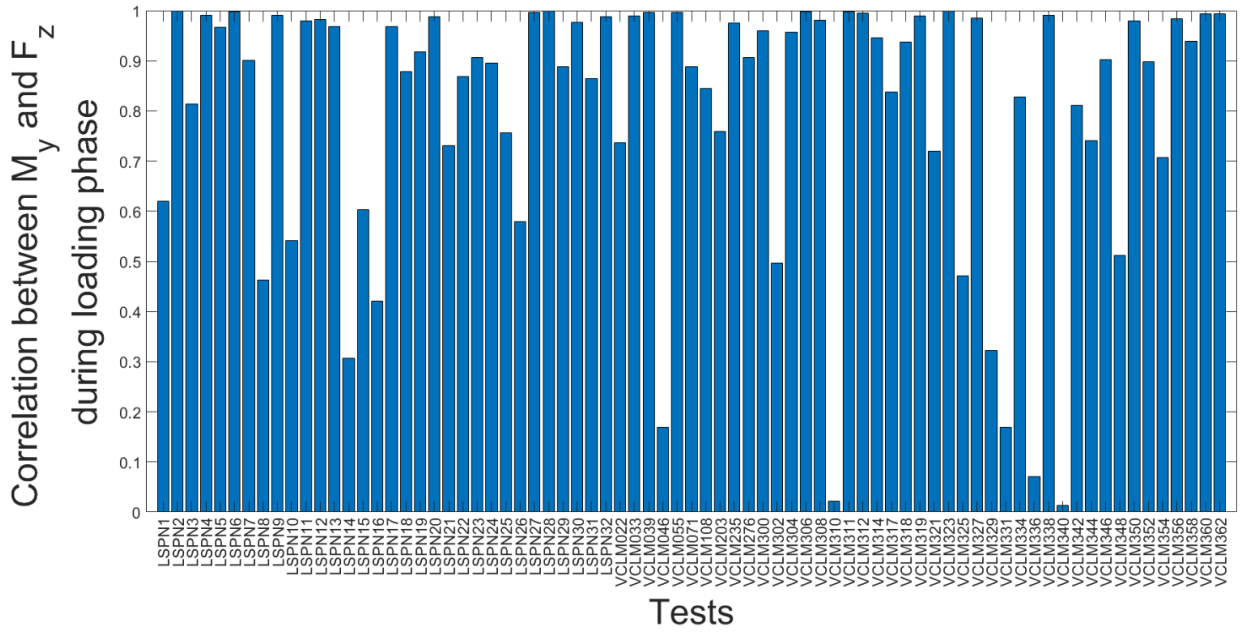

Figure 1. Correlation of F_z and M_y for Duke and Medical College of Wisconsin (MCW) lumbar tests for LS-05. The majority of the tests show highly correlated data owing to differences between the effective moment center of the loading event and the estimated geometrical center of the T12-L1 intervertebral disc.

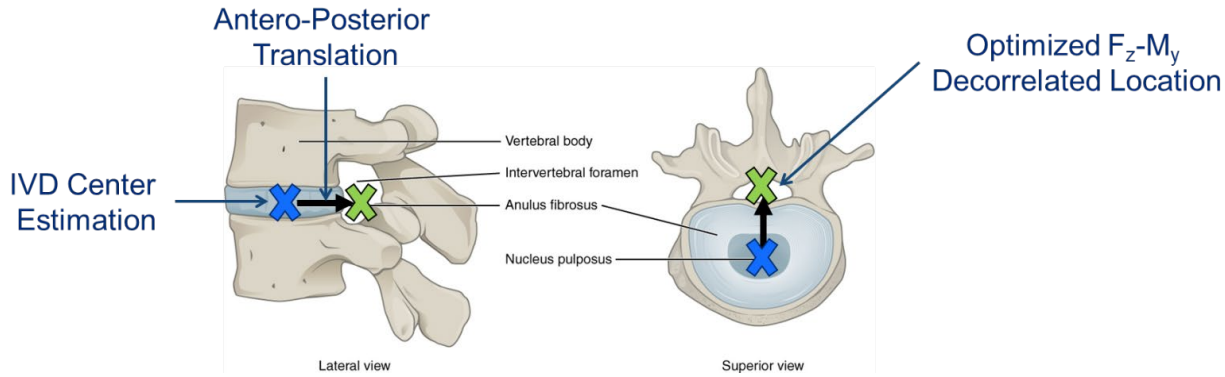

Figure 2. Optimized moment arm (antero-posterior translation) of F_z-M_y decorrelated moment based on reduction of cross-correlation between M_y and F_z during loading to first major failure. Example from recent LS-05 lumbar injury risk HIPC.

To give a simple example for a prismatic beam (Figure 1), a pure axial load measured off of the central axis will have an “apparent” peak moment My,measured that is a function of the axial force Fz,measured and the distance from the measurement point to the center of the section of the spine, here assumed to be a prismatic beam. In the recent LS-05 testing at both MCW and Duke, the assumed location of the transferred moments was the center of the intervertebral disc, which is not the location of the section center if the spine is assumed to be approximated by a prismatic beam. For pure vertical loading injury criteria, this is not an issue since Fz,measured=Fz,alt=Fz,centered. However, for

combined injury criteria that included moment, in the limiting case of pure axial applied force, there will be an apparent peak moment at the alternative location in the prismatic beam Fz,measured*dx,alt (Figure 3A) that is nonzero. In contrast, at the center of the section, the Fz,measured*dx,centered=0 for the pure axial force case and does not contribute to the stress to failure (Figure 3B).

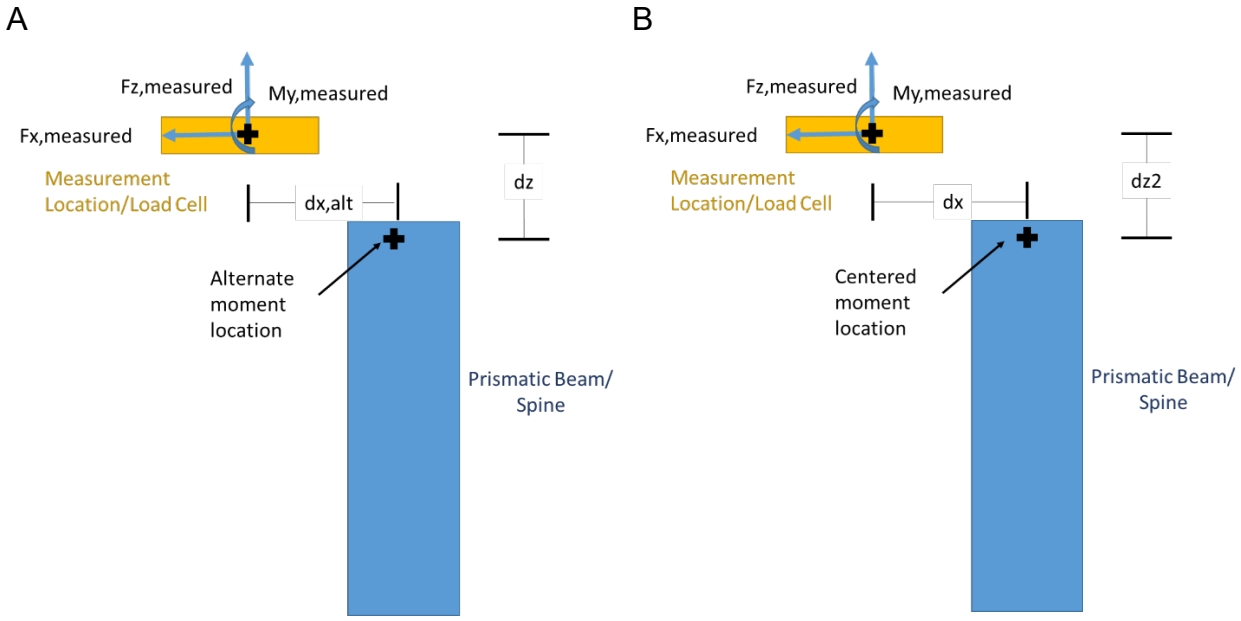

Figure 3. Illustration of moment translation in the pure axial loading limit. A. 2D representation of the "original vertebral disc translation" site. B. Representation of the desired "section center translation" site. Bilateral symmetry is assumed in all joint translations.

If an injury criterion was developed using a combined criterion for the circumstance using the alt location, the eventual criterion would have more contribution from Fz through both Fz,alt and the apparent My,alt than would contribute to local stress values. This contribution would increase based on distance to the actual center of the section and would bias the small beams relative to large beams in the injury risk value. This contribution can be large. For example, a 5-mm variance in dx can produce an apparent My of 250 Nm under a 5-kN pure axial load that does not contribute to stress to failure in the desired section or in the comparable prismatic beam.

To mitigate the influence of apparent, and not actual, moments on a combined criterion that assumes a prismatic beam approach with large axial forces, there are three potential approaches. The first would be to estimate the actual section center of the spine at the desired spinal level (here, T12-L1 joint center) and simply translate from the T12-L1 disc center. This approach, unfortunately, has substantial limitations, owing largely to inaccuracies in estimating the relevant section that is under load that would increase the intrinsic variance of the test results. Another approach would be to estimate the local cross-sectional area of loading in the disc at the disc center, which

would include both disc and posterior spinal elements. Even given that bilateral symmetry is a reasonable assumption based on structural geometry of normal lumbar spines, this estimate is sensitive to both the section selected and the assumptions of what part of the image contributes to the loading. Issues include the following:

- The full disc area cannot contribute to the loading in the same way the smaller full vertebral cross section would contribute to axial and moment support.
- Determining the appropriate section angle that preserves the desired anatomical level to be assessed based on some combination of disc and posterior elements. The loading area, and hence the assessment of dx is sensitive to this measure for large applied compressive loads.

A final approach is to determine the moment center based on decorrelating the F_z and My time histories using the moment arm dx (Corr(F_z(t), M_y(dx, t)) is minimized over a relevant time interval). It is clear that this is an exact procedure given pure axial loading, which will result in a dx that is located in the center of a homogeneous prismatic beam, and My,centered is zero at the center for all time. Similarly for applied forces/moments that result in large F_z and nonzero My at the center of the section, it is clear that this procedure will also result in accurate dx for the given time histories. Both positive and negative correlations between M_y(t) and F_z(t) will produce dx estimates to either the anterior or posterior of the desired section center, and the minimized correlation will produce a “moment center” where the remaining M_y contributes to the failure stress in the section. This analysis was performed by calculating the correlation between F_z and M_y and minimizing this correlation by changing the location of the forces in the x direction (dx) using Equation 1.

The principal limits to this approach are as follows:

- The limitations of the prismatic beam approach for spines. It is clear that, in general, spines do not have the same rotational stiffness or failure forces/moments in the anterior and posterior direction. However, the dataset used involves predominantly anterior loading of the lumbar spine under relatively large axial loads. This mitigates some of this limitation. Further, the ATD behaves more like a prismatic beam, increasing the value of this approximation in transferring the cadaver injury criteria (HIPC) to the ATD (IARC).
- The approach assumed large axial forces are the predominant source of stress in the spine and that conditions never approach “pure moment” conditions. This is supported by the axial force results from the tests, even in the “extreme” postures considered in this series.

2.2. Injury Censoring

An example of typical injury censoring is taken from the recent LS-05 HIPC study for WIAMan. This injury criteria were developed for single- or multi-level vertebral body fracture. Out of the 75 tested specimens, 64 resulted in a single- or multi-level vertebral body fracture, 9 resulted in other injury types (e.g., spinous process fractures), and 2 resulted in no injury.

The 11 noninjury tests were defined as right censored at the maximum axial force during the loading phase of the test. For a failure test, the interval censoring used sensor data to identify the lower and upper bounds, with the lower bound being the identified initiation of fracture and the upper bound being the maximum force of the loading phase. To identify fracture initiation, acoustic emission results were supplemented by identifying major changes in the response of the strain gauges. The acoustic sensors are more sensitive than the strain gauge to low-level bony fractures, therefore the acoustic sensors showed evidence of bone fracture earlier or at the same time than the strain gauge (Figure 4). The earliest times are used for determining the lower bound of the censoring interval. In some cases, the noise floor prevented the use of acoustic signals for fracture identification. However, where available, the acoustic sensors are consistent with the fracture assessment, and the strain gauge data was available for fracture identification for the remainder of the tests.

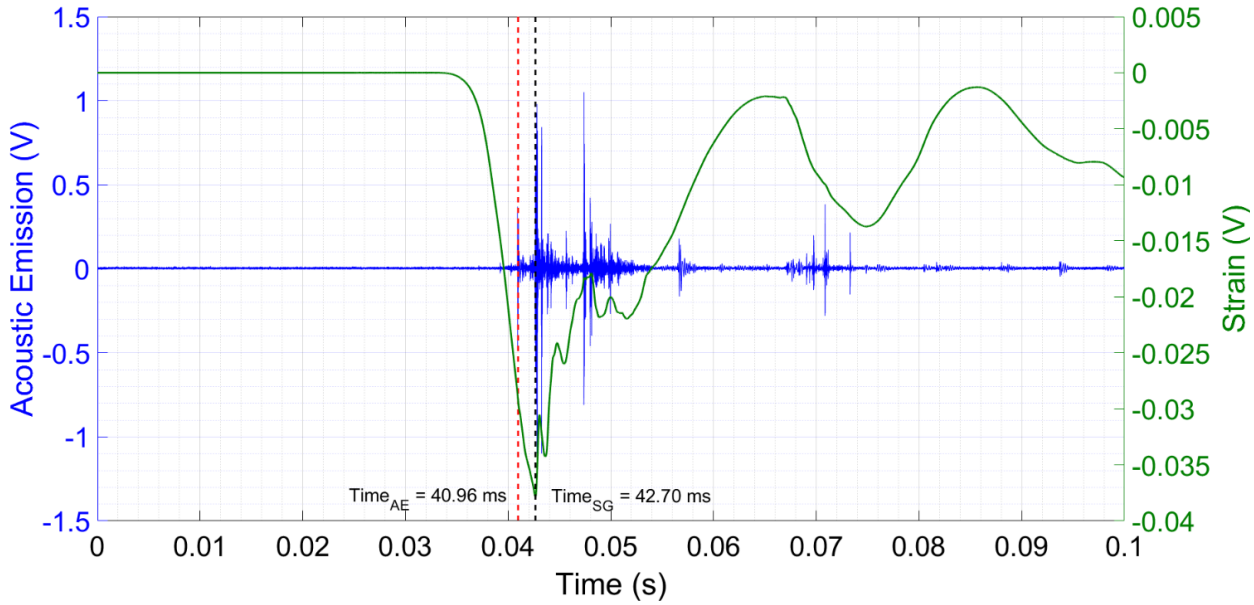

Figure 4. Example of fracture initiation determination for lower bound of censoring interval for Duke test LSPN31. Blue trace corresponds to band pass filtered (100–1000 KHz) acoustic emission of L2 sensor. Green trace represents L2 strain gauge measurement. Initiation of acoustic emission (red dashed line) indicated by acoustic signal above a 0.25-V threshold at 40.96 ms. Strain gauge fracture indication (dashed black line) coincides with acoustic emission threshold of approximately 1 V at 42.7 ms.

2.3. Combined Injury Metric

For the example LS-05 tests, a combined loading injury metric criteria of the peak axial force (Fz) or peak sagittal resultant force (Fr) at the T12-L1 moment center and bending moment at T12-L1 (My) was used to incorporate the contributions of both the bending moment and force(s) to the injury outcome in the range of tested nominal postures. This allowed the combination and inclusion of the entire Duke and MCW lumbar data sets. The combined loading injury metric was based on prismatic beam failure analysis (Figure 5), similar to that used by the U.S. Department of Transportation for assessment of the Hybrid III ATD neck in crash testing.[8] This formulation, an exact injury criterion for nonlinear prismatic beams, incorporates force and moment as

$$\kappa = \frac{F_Z}{F_{z,\,crit}} + \frac{M_y}{M_{y,crit}} \tag{2}$$

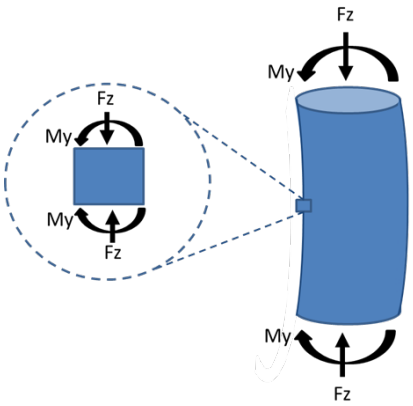

$$I = \frac{\sigma_{F_z}}{\sigma_{F_{z,crit}}} + \frac{\sigma_{M_y}}{\sigma_{M_{y,crit}}}$$

$$I = \frac{F_z}{F_{z,crit}} + \frac{M_y}{M_{y,crit}}$$

Figure 5. Combined loading stress and force failure criteria based on prismatic beam formulation

Based on the assumptions, independent force and moment contributions taken at each instant of time produce independent stress contributions to assessed failure. The force contributions, Fz or Fr, contribute across the section, while the moment contribution, My, contributes positive stress at the anterior or posterior surface with negative stress at the opposite side, depending on the direction moment contribution. In the analyses for the combined injury criteria, the testing largely resulted in anterior spinal compression moment contributions. Since there was insufficient injury testing to assess independent posterior and anterior compressive loads, spinal injury was assumed to be symmetric in the anterior and posterior surfaces.

2.4. Injury Probability Curve and Combined Metric Optimization

Typical parametric distributions are available to assess survival analysis risk functions. These are often more convenient than the comparable and more exact non-parametric forms since the distributions are smooth in the independent variable(s), allowing risk estimation without abrupt jumps in the assessed risk that will discontinuously affect tradeoff analyses. The cost of the use of parametric models is an assessment of model and distribution fit.

In the WIAMan LS-05 risk function development, three distribution functions (Weibull, Log-logistic, and Lognormal) were evaluated for the development of both an axial loading and combined loading (L_{ic}) injury risk. These distributions were chosen based on comparison with a previous study.[14] For the axial loading injury criteria, both the axial force (F_z) and the resultant sagittal force (F_r) at T12 were evaluated as biometrics for injury prediction due to their expected link to lumbar spine fracture and the advantage of being proximal to the thoracolumbar junction.

For combined assessment, there is a peak (or κ) in a given test, but it depends on Fz,crit (or Fr, crit) and My,crit in Equation 2, which are not known initially. Ideally, these would be estimated from tests with nearly pure axial loading (all F_z, no or little M_y) and from tests with nearly pure bending loading (all M_y, no or little F_z). However, an alternative approach is to optimize for confidence interval, or normalized confidence interval size (NCIS), which would presumably be minimized by a series of tests using pure moment, pure axial force, and combined loading. This quantity is defined as

$$NCIS = \frac{UB_p - LB_p}{M_p} \tag{3}$$

where UB_p is the upper bound of the injury probability curve, LB_p is the lower bound, and M_p is the mean metric value. To minimize the NCIS, an initial value of $F_{z,crit}$ (or $F_{r,crit}$) and $M_{y,crit}$ were assumed, and a κ metric is calculated for the failure tests at the maximum values of the metrics. Subsequently, the κ metric was calculated with known nonfailure points based on acoustic emission and strain response sensor evidence of nonfailure. With the previously calculated κ values, a risk function L_{ic} (through the aforementioned distribution functions) and the NCIS were determined. Posteriorly, $F_{z,crit}$ (or $F_{r,crit}$) and $M_{y,crit}$ were changed based on a line search algorithm,[15] and the process was repeated until the calculated κ metric minimized the NCIS across risk levels from 1% through 99%. The procedure can be described as follows:

1. Start with an initial value of $F_{z,crit}$ (or $F_{r,crit}$) and $M_{y,crit}$. Note that the normalizations of $F_{z,crit}$ (or $F_{r,crit}$) and $M_{y,crit}$ are set by the assumption that the 50% risk in the final risk assessment occurs at a value of κ = 1. This makes the variable the ratio between $F_{z,crit}$ (or $F_{r,crit}$) and $M_{y,crit}$.
2. Calculate κ for the failure tests to find the maxes.
3. Calculate κ for known nonfailure points based on acoustic and strain gauge data and find nonfailure values.
4. Calculate risk function based on interval censoring 2 and 3. Keep in mind to maintain right-censored and interval-censored points according to the proposed vertebral body injury criteria.
5. Change $F_{z,crit}$ and $M_{y,crit}$ based on line search algorithm.
6. Repeat 2–5 until κ minimizes the desired NCIS value (Equation 3). This can be selected as any NCIS for a given risk or across a region of the curve or across the entire set of κ values. Here, the minimal value is selected using the integrated NCIS across the computed risk calculation at that step from a risk of 0.01 to a risk of 0.99.

For the selected lognormal distribution from LS-05, the location (μ) and scale (σ) parameters were determined to be –0.0578 and 0.3215, respectively. The combined injury criteria are then defined by Equation 4. The critical parameters were optimized to $F_{r,crit}$ = 5824 N and $M_{y,\,crit}$ = 1155 Nm (Equation 5).

$$\mathrm{L}_{ic}(\kappa; -0.0578, 0.3214) = \frac{1}{2} + \frac{1}{2} \cdot \mathrm{erf}\left(\frac{\ln(\kappa) - 0.0578}{0.3214 * \sqrt{2}}\right) \tag{4}$$

$$\kappa = \frac{F_r}{5824} + \frac{M_y}{1155} \tag{5}$$

3. LUMBAR SPINE VERTEBRAL BODY FRACTURE IARC

The LS-05 IARC was developed following energy equivalency methods as previously developed with a single injury metric (axial force/resultant force). The assumption is that the energy to failure with stress contributions from both the moment and the axial or resultant force will be the same for the ATD and cadaver. For hyperelastic prismatic beams, one with failure (cadaver) and one without failure (ATD), this correspondence in energy is exact to the desired point of failure in the cadaver. The approach eliminates the issue with matched pair tests in that a given (and arbitrary) energy input greater than the fracture injury in the cadaver under axial loading will always produce higher corresponding forces and moments in the ATD than is appropriate for use with the cadaver since the cadaver breaks and the ATD does not under design loads. This ensures that all energy input in the cadaver above the failure force and moment values is not represented in the risk function that should be transferred to the ATD. In the ATD, however, the forces and moments may increase without bound, depending on the energy level selected for the matched pair test, not on the cadaver failure energy.

The energy equivalency for a single input metric is straightforwardly outlined, as only the desired metric (for example, Fz, Fr for the LS-05 analysis) needs to be matched at an isoenergy level. The current methodology uses an expanded IARC to include the moment contribution to the injury risk (i.e., develop the combined metric for the ATD at isoenergy levels).

3.1. Energy Equivalency for a Single Input Metric

Traditional translational methods used to develop an ATD IARC from a PMHS HIPC such as match-paired testing or perfect biofidelity rely on the capability of the ATD to mimic the behavior of the human spine under the appropriate loading and boundary conditions. The degree of biofidelity is limited by constraints and design requirements. However, there are two principal potential differences between ATDs and cadavers that limit the usefulness of matched pair testing. First, the ATD and cadaver may have different intrinsic stiffnesses in the desired loading direction, making force or displacement estimates not comparable. Second, ATDs are generally designed to be robust to failure loading in the cadavers. This ensures that for a given failure loading scenario in the cadaver, the resulting paired ATD forces will be higher under nearly every circumstance barring the laborious determination of input conditions for incipient failure in the cadavers, which are then used to provide matching ATD test conditions

Matching a metric—a force, for instance—for human and ATD responses leads to an overestimation of the injury reference value due to the differences in mechanical work to failure (human) or to peak force (ATD) (Figure 6).

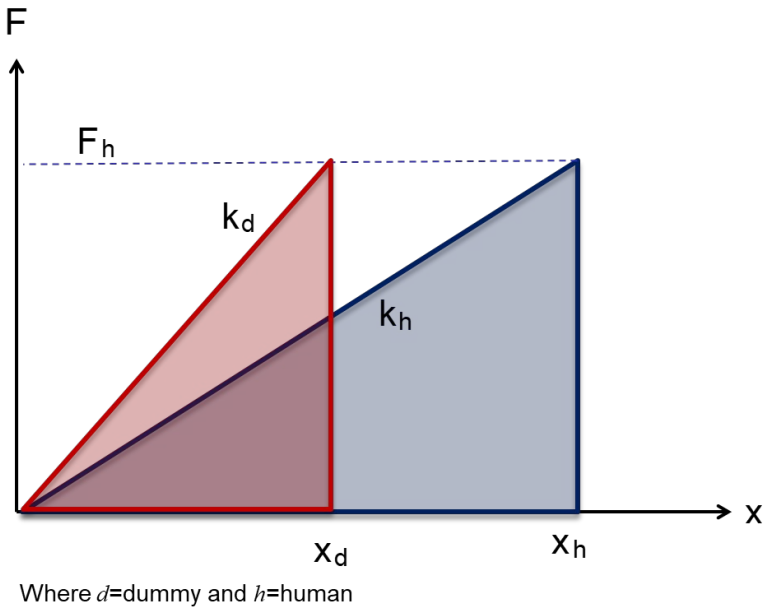

Figure 6. Linear elastic scaling at equal force. Note that the mechanical work (area under the curve) for the ATD and human differ at the same force value.

Similarly, when matched to failure displacement the mechanical work performed by the human and ATD is different (Figure 7). This linear stiffness scaling alone is not enough to capture the appropriate amount of energy that was introduced to the system to cause failure.

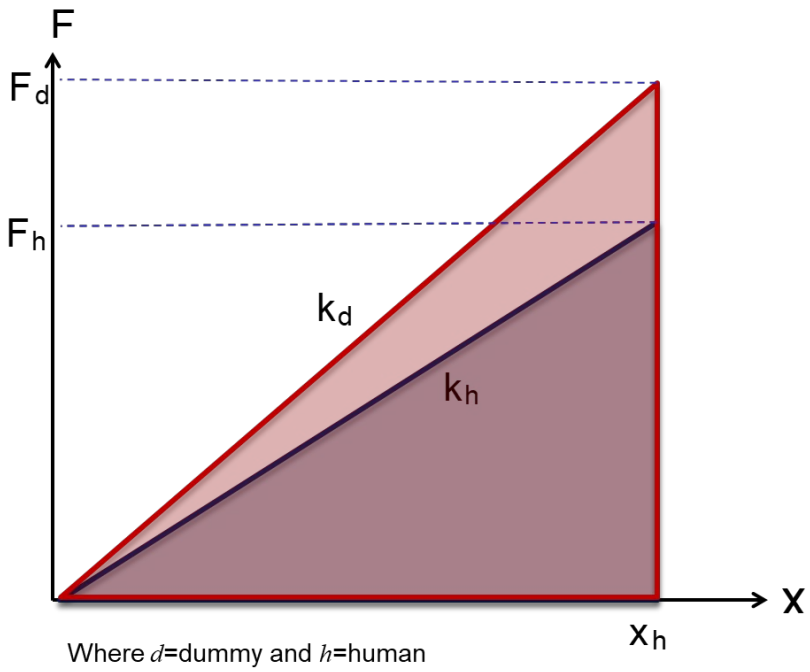

Figure 7. Linear elastic scaling at equal displacement. The mechanical work for the ATD and human differs.

The second critical limitation of traditional match-paired testing is the capability of the ATD to be robust to failure for comparable cadaver failure points and to measure forces and moments beyond the cadaver failure point (Figure 8). While match-paired testing can allow a direct correlation of measured ATD responses to PMHS injury outcomes, these increased forces and moments relative to those of the cadaver result in an overestimation of the injury tolerance.

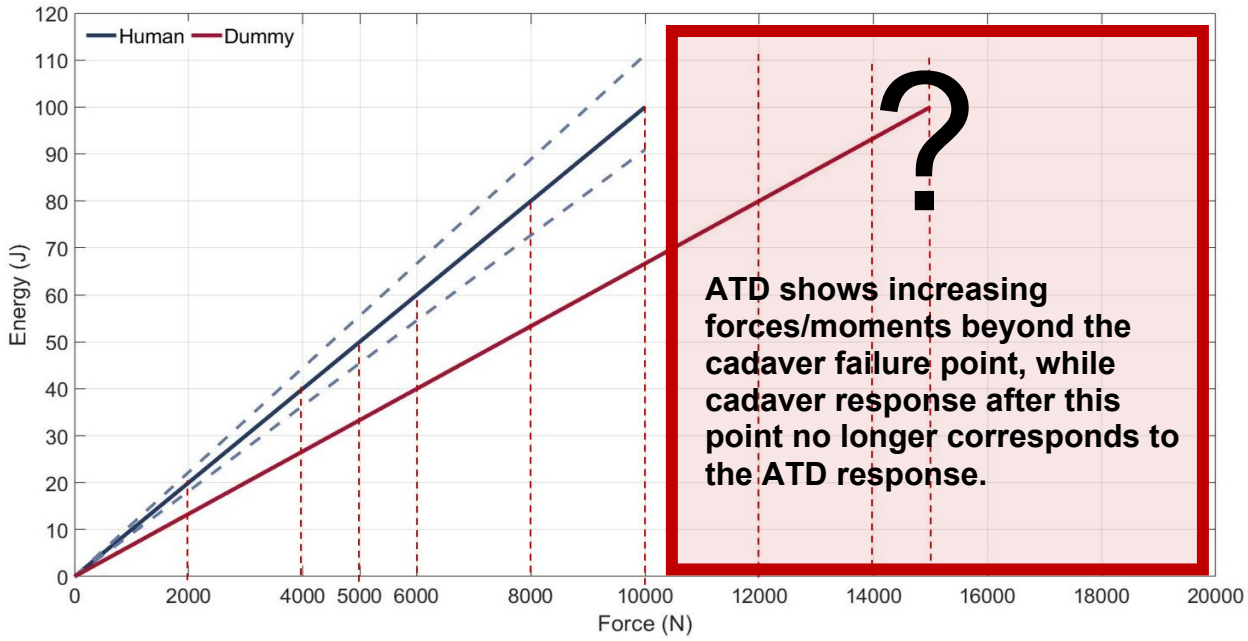

Figure 8. Linear elastic isoforce equivalency method on generic dataset for HIPC to IARC translation

The consequence of this in match-paired testing is that energy or velocity inputs are generally chosen to be convenient values, not based on incipient fracture of the cadavers. So, a given energy input that produces cadaver failure, limiting peak forces or stresses in the cadaver, will produce a force or stress in the ATD that is always higher by an arbitrary amount that depends on the selected energy input (Figure 9). This is true even if the ATD and the cadaver have identical stiffnesses under the loading conditions. This shifts the injury risk assessment to the right (i.e., to higher values of the metric) (Figure 9, right), resulting in an overestimation of the injury metric for a given injury risk value, and an underestimation of risk for a given cadaver equivalent metric. The amount of overestimation of the metric is generally based on how much energy is input to the ATD system beyond cadaver failure.

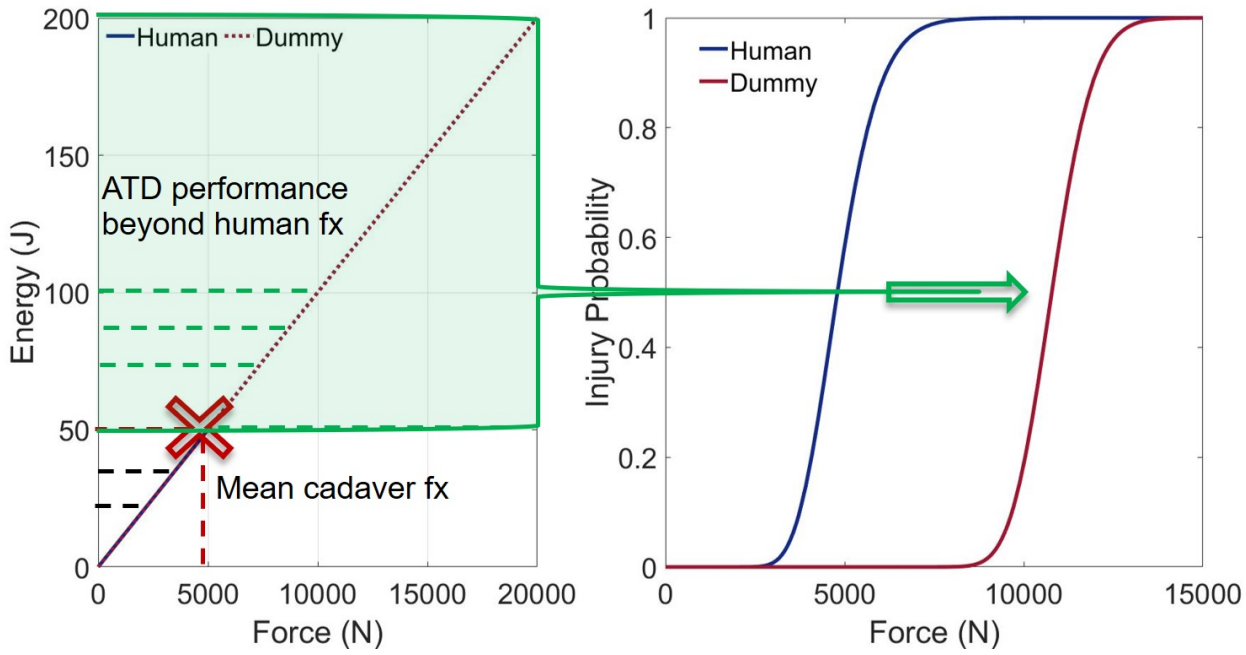

Figure 9. Force-Energy response and injury risk curve through the traditional match-paired method. The use of a robust ATD in matched conditions where the cadaveric surrogates failure leads to an overestimation of the comparable injury metric at a given risk or an underestimation of risk for a given injury metric.

A strain energy equivalency approach overcomes these limitations. The strain energy is the result of the scalar product of two vectorial quantities, the force and internal displacement or strain in the cadaver or ATD (Equation 6), and as such it is independent of the system where it is determined (i.e., invariant) with

$$E = \int F_z \cdot dz \tag{6}$$

In the LS-05 tests, F_z is typically a mass-compensated load cell value (unaffected by acceleration) and dz is a strain measure. Examples include the displacement of the lumbar spine T12/L1 joint relative to the L5/S1 joint or incremental piston displacement measured by the linear variable differential transformer in force test machine testing. For a simple linear elastic scaling model,

$$F = k * x \tag{7}$$

$$E = \frac{1}{2} F * x = \frac{1}{2}\, k * x^2 \tag{8}$$

Equating for isoenergy scaling as defined by Figure 10:

$$E = \frac{1}{2}k_h x_h^2 = \frac{1}{2}k_d x_d^2 \tag{9}$$

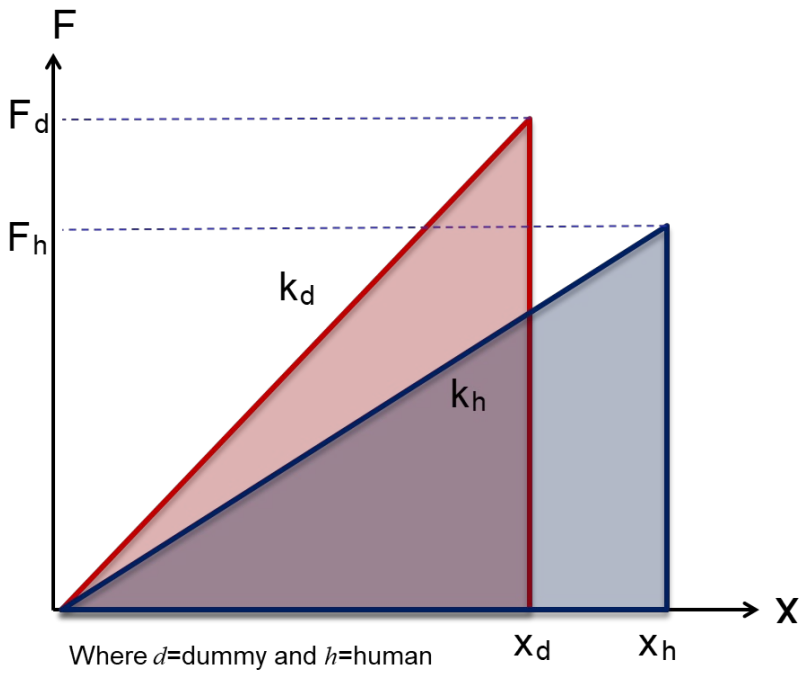

Figure 10. Scaling for a linear elastic model at isoenergy

By characterizing the cadaver and ATD energy response in terms of force (Figure 11), we can determine the equivalent response between cadaver and ATD at isoenergy. The transfer function obtained during an isoenergy translation (Figure 12) can then be used to develop the ATD IARC by determining the corresponding injury points across the PMHS and ATD.

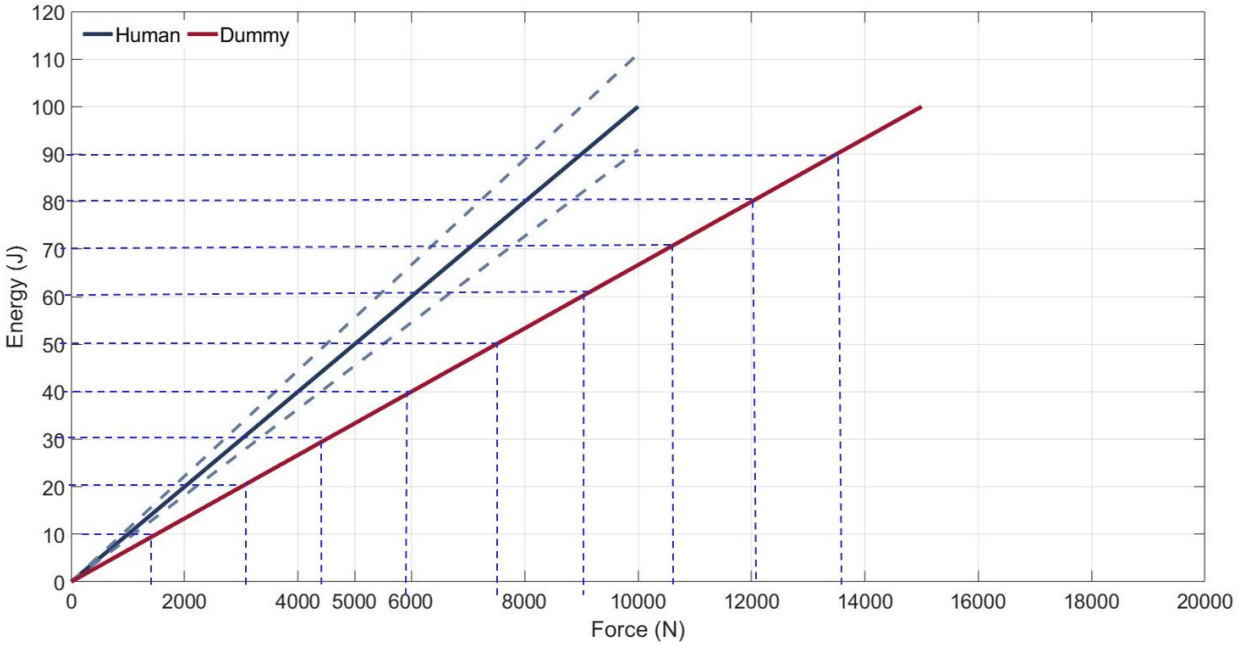

Figure 11. Linear elastic isoenergy equivalency of PMHS and ATD response on generic dataset

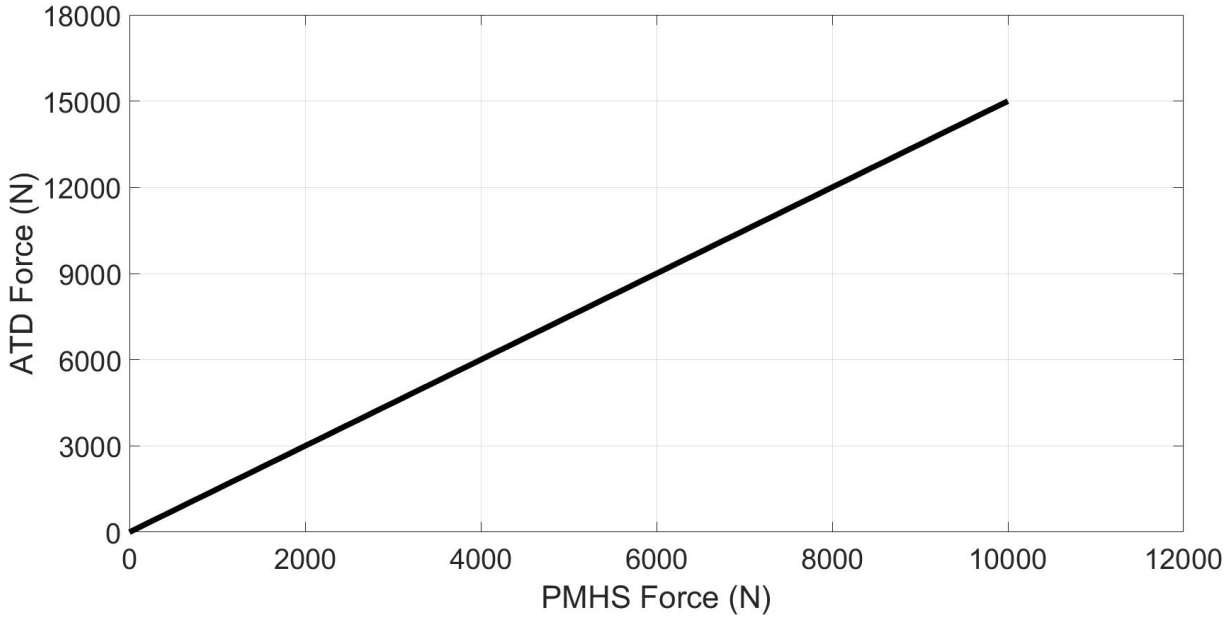

Figure 12. Cadaver to ATD transfer function at isoenergy for a generic dataset

The injury risk (IARC) for the ATD can then be determined by matching the PMHS injury risk at a given force with the corresponding ATD force given by the isoenergy transfer function.

3.2. Moment Contribution

This approach may be expanded to include moment using the analogous expressions for moment energy (Equation 9) defined as

$$E_M = \frac{1}{2}\, b_h \theta_h^2 = \frac{1}{2}\, b_d \theta_d^2 \tag{10}$$

with the sub-indices *h* and *d* referring to the cadaver and ATD, respectively.
To account for the moment contribution to the system's energy, based on prismatic beam failure theory and similarly to the proposed HIPC combined metric, the energy of the system is defined as the sum of the force strain energy contribution and the moment strain energy contribution, defined as

$$E = E_F + E_M = \frac{1}{2}\, k_h x_h^2 + \frac{1}{2}\, b_h \theta_h^2 = \frac{1}{2}\, k_d x_d^2 + \frac{1}{2}\, b_d \theta_d^2 \tag{11}$$

This is a point estimate for the energy, and both the displacements for the force (x_h) and the moment (θ_h) are estimated using cross-head motion and geometric constraints. Since the cadaver and ATD are nonlinear, the strain energy for both force and moment is calculated using the point estimate in Equation 11 by the integral form as

$$E = E_F(t) + E_M(t) = \int \frac{1}{2}\, k_h x_h^2(t)dt + \int \frac{1}{2}\, b_h \theta_h^2(t)dt = \int \frac{1}{2}\, k_d x_d^2(t)dt + \int \frac{1}{2}\, b_d \theta_d^2(t)dt \tag{12}$$

Since the cadaver energy contribution has been reduced to a single risk assessment parameter, κ as described, there is an association between this value κ(My, Fz) and energy based on Equation 12.

To make the translation for the ATD in a manner analogous to the previous force-only injury assessments, a surface in 3D (*Fz or Fr, My, E*) is needed that describes all of the energy values for the ATD lumbar response as a function of force/moment pairs accessible during testing of ATD components. To obtain this surface, additional test conditions were performed to expand the range of ATD values of available *Fz or Fr*, and *My*. Especially desirable were larger values of *My* relative to *My,crit* to expand the relevant range of ATD risk assessments outside the nominal postures. Given the anatomic variability of the cadaver testing and the consistency of the repeated ATD tests in the original range of postures, higher values of *My/My,crit* were present in the cadaver dataset.

So, to perform the mapping from cadaver to ATD,

1. A surface in 3D was interpolated using the ATD tests at all postures giving the widest range of *Fz or Fr, My, E* triplets, where *E(Fz or Fr, My).* Energy values on this surface were assumed to correspond to the energy values represented in the cadaver HIPC single parameter *k*.
2. A 3D optimization was performed to find the energy from the cadaver HIPC that corresponded to an *Fz or Fr, My* doublet from the ATD testing on the ATD surface plot. Note that this optimization produces a monotonically increasing energy line on the surface that provides the comb values for the ATD IARC.

The mapping was performed at isoenergy levels (Figure 13). It was assumed that the injury metric ratio (κ) behaved equally between cadaver and ATD response. At a given cadaver energy level, the Fr/My ratio is defined through the average energy equivalent responses of the ATD to the extended IARC posture testing.

Given this technique, the cadaver HIPC may be translated to an ATD IARC pointwise including confidence intervals, if desired. Since the cadaver variance and confidence intervals are generally much larger than repeatable ATD components, it is often sufficient to translate the cadaver confidence intervals to the IARC neglecting the ATD without effect at the 5% level. At this point, the resulting IARC does not likely fit a parametric distribution, and a suitable distribution or function fit may be matched to the pointwise estimate to as much accuracy as desired.

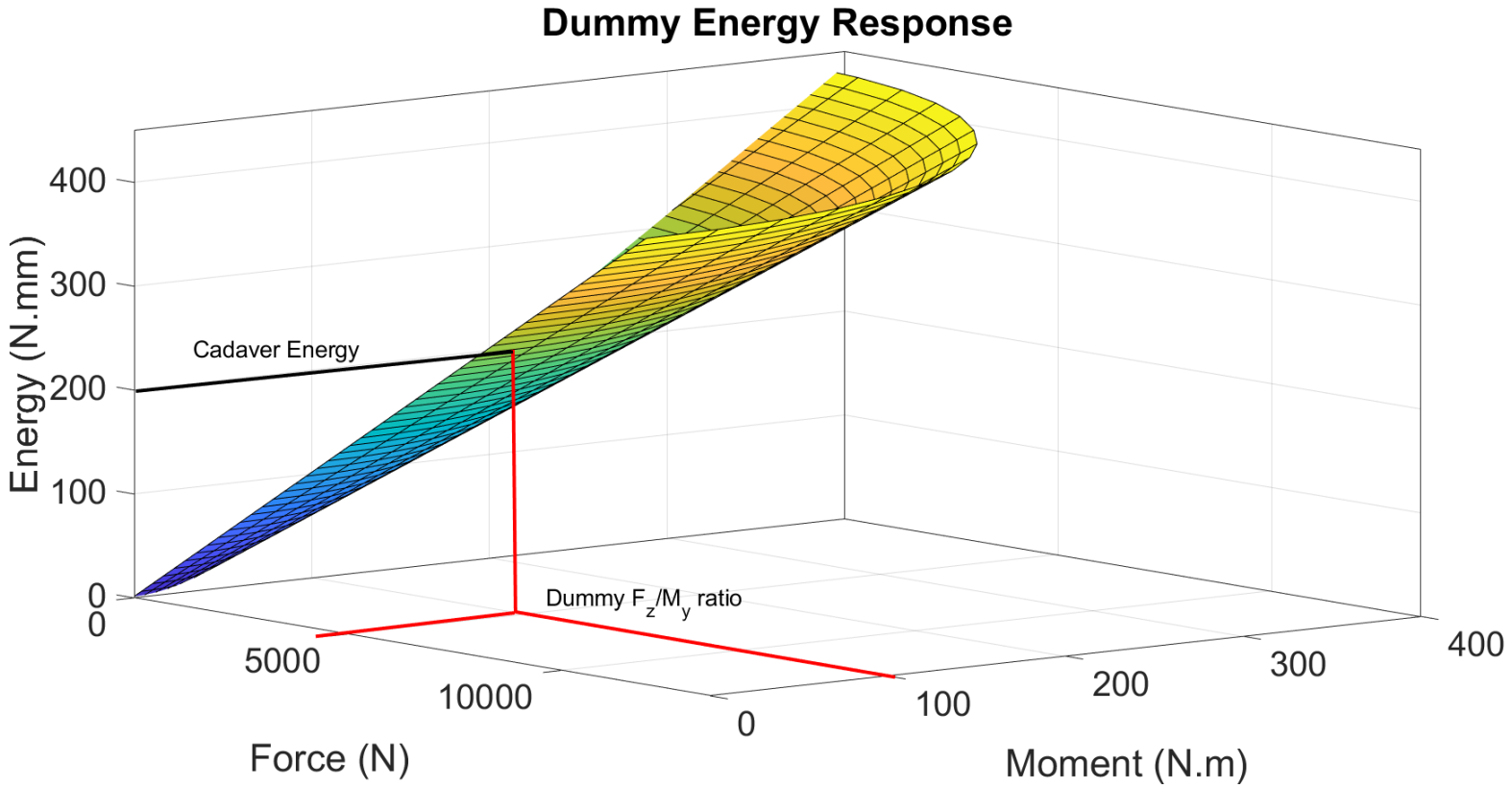

Figure 13. Example of surface plot of Force (*Fz or Fr*) and Moment (*My)* vs Energy for cadaver energy response extrapolation

4. CONCLUSIONS

Determining and refining injury reference parameters for both human and ATD are central applications of injury biomechanics to inform the design and development of injury-mitigating devices and techniques. Several injury criteria have been established in the literature, from body responses during automotive crashes to head, cervical spine, foot-ankle complex, and thoracic injury tolerance,[4,8,12,16,17] among others. Fewer studies have looked into the injury risk of the lumbar spine during dynamic loading,[13] with its translation to ATD injury reference values and combined loading metrics effects receiving even less attention.

This work outlines a methodology to develop both human injury risk probability curves and ATD injury assessment reference curves that accounts for the influence of combined loading (axial and bending) for the HIPC and translates it through an isoenergy method to establish an equivalent ATD IARC.

The development of the HIPC is based on the failure criteria for prismatic beams used to establish previous injury criteria.[8] The approach uses a decorrelation process to eliminate the contributions of spurious moments that are introduced in the system by load translation between the sensing elements of the test rig and the actual moment center, hence allowing the determination of the appropriate individual contributions of the axial force and bending moment to the injury assessment (moment center). The critical values for the combined metric that are defining of the injury criteria are determined through an optimization process that minimizes the normalized confidence interval across the risk assessment. The methodology proposed for the HIPC can be extended to any data set under bending and axial loading conditions.

Once the HIPC is determined, the ATD IARC is developed by means of a transfer function developed under isoenergy conditions across the PMHS and the ATD. The transfer function is developed by defining the energy response of PMHS and ATD as a function of both force and moment so that energy = $E(F_z,M_y)$. This definition will result in a 3D surface that defines the energy in terms of an F_z/M_y (κ) pair as shown in Figure 12. The energy response of the PMHS, dependent of the F_z/M_y pair, is used to map the corresponding κ_{PMHS} values to the κ_{ATD} values, assuming that the pair behaves in the same manner across ATD and PMHS. Meaning, at a given κ_{PMHS} there is an injury risk and an energy value for the cadaver, the injury risk is associated to an energy response through the PMHS pair, and, at the same energy-injury risk level, the ATD pair is determined through the ATD $E(F_z,M_y)$ response. The IARC isoenergy development method can then be achieved by the following steps:

1. Obtaining the energy as a function of the F_z/M_y (κ) pair for both cadaver and ATD through experimental testing.
2. Determining the pair associated to an injury risk in the cadaver from the developed HIPC.
3. Using the 3D surface obtained in step 1 for the cadaver to determine the energy level for the pair that is associated with an injury risk level.
4. Using the 3D surface established in step 1 for the ATD and the energy associated to the injury risk value obtained in 3 to determine the corresponding ATD F_z/M_y (κ) pair.

The ATD pair determined in 4 will have the same injury risk value that was determined in 3.

The HIPC confidence intervals are transferred to the ATD using the same procedure. The energy values associated with the upper and lower confidence interval are calculated and transferred to the ATD surface as detailed previously. In the current analyses, the ATD experimental variance is neglected since ATD experimental response is generally repeatable to within 1%, providing a small overall contribution to the experimental confidence intervals. This general approach avoids the overestimation injury metrics for a given risk value that is inherent in the traditional use of the matched pair procedure.

5. REFERENCES

1. Foster, J., Kortge, J., & Wolanin, M. (1994). Hybrid III-a biomechanically-based crash test dummy. In S. H. Backaitis and H. J. Mertz (Eds.), *Hybrid III: the first human-like crash test dummy* (pp. 49–64). Society of Automotive Engineers, Inc.

2. Mertz H., Irwin, A., Melvin, J., Stanaker, R., & Beebe, M. (1989). *Size, weight and biomechanical impact response requirements for adult size small female and large male dummies* (SAE Technical Paper). SAE International.

3. Mertz, H. J., Horsch, J. D., Horn, G., & Lowne, R. W. (1991). Hybrid III sternal deflection associated with thoracic injury severities of occupants restrained with force-limiting shoulder belts. *SAE Transactions*, 1108–1122.

4. Mertz, H. J., Prasad, P., & Nusholtz, G. (1996). Head injury risk assessment for forehead impacts. *SAE Transactions*, 26–46.

5. Nightingale, R. W., McElhaney, J. H., Camacho, D. L., Kleinberger, M., Winkelstein, B. A., & Myers B. S. (1997). The dynamic responses of the cervical spine: buckling, end conditions, and tolerance in compressive impacts. *SAE Transactions,* 3968–3988.

6. Nyquist G., Begman, P., King, A. I., & Mertz, H. J. (1980). Correlation of field injuries and GM hybrid III dummy responses for lap-shoulder belt restraint. *Journal of Biomechanical Engineering*, *102*, 103–109.

7. Yoganandan, N., Pintar, F., Maiman, D., Cusick, J., Sances, A. Jr., & Walsh, P. (1996). Human head-neck biomechanics under axial tension. *Medical engineering & physics*, 18, 289–294.

8. Eppinger, R., Kleinberger, M., Kuppa, S., Saul, R., & Sun, E. (1998). *Development of improved injury criteria for the assessment of advanced automotive restraint systems*. National Highway Traffic Safety Administration.

9. Mertz, H. J., Prasad, P., & Irwin, A. L. (1997). Injury risk curves for children and adults in frontal and rear collisions. *SAE Transactions,* 3563–3580.

10. Pintar, F. A., Yoganandan, N., Sances, A., Reinartz, J., Harris, G., & Larson, S. J. (1989). Kinematic and anatomical analysis of the human cervical spinal column under axial loading. *SAE Technical Paper*.

11. Prasad, P. & Daniel, R. P. (1984). A biomechanical analysis of head, neck, and torso injuries to child surrogates due to sudden torso acceleration. *SAE Transactions*, 784–799.

12. Poplin G. S., McMurry, T. L., Forman, J. L., Ash, J., Parent, D. P., Craig, M. J., Song, E., Kent, R., Shaw, G., & Crandall, J. (2017). Development of thoracic

injury risk functions for the THOR ATD. *Accident Analysis & Prevention*, 106, 122–130.

13. Yoganandan, N., Moore, J., DeVogel, N., Pintar, F., Banerjee, A., Baisden, J. L., Zhang J., Loftis, K., & Barnes, D. (2020). Human lumbar spinal column injury criteria from vertical loading at the base: Applications to military environments. *Journal of the Mechanical Behavior of Biomedical Materials*, 103690.

14. Yoganandan, N., DeVogel, N., Moore, J., Pintar, F., Banerjee, A. Zhang, J. (2020). Human lumbar spine responses from vertical loading: ranking of forces via Brier score metrics and injury risk curves. *Annals of Biomedical Engineering*, 48, 79–91.

15. Wolfe, P. (1969). Convergence conditions for ascent methods. *SIAM Review,* 11, 226–235.

16. Funk J. R., Crandall J. R., Tourret L. J., MacMahon, C. B., Bass, C. R., Patrie, J. T., Khaewpong, N., & Eppinger, R. H. (2002). The axial injury tolerance of the human foot/ankle complex and the effect of Achilles tension. *Journal of Biomechanical Engineering*, 124, 750–757.

17. Hubbard, R. P. & McLeod, D. G. (1974). Definition and development of a crash dummy head. *SAE Transactions*, 3836–3851.

Appendix A – List of Acronyms

ATD	anthropometric test device
DAC	Data & Analysis Center
DEVCOM	U.S. Army Combat Capabilities Development Command
HIPC	human injury probability curve
IARC	injury assessment reference curve
IARV	injury assessment reference value
MCW	Medical College of Wisconsin
NCIS	normalized confidence interval size
PMHS	postmortem human subject

Appendix B – Distribution List

ORGANIZATION

U.S. Army DEVCOM Data & Analysis Center
FCDD-DAD-TP/G. Dietrich
FCDD-DAG-S/K. Loftis
FCDD-DAG-S/K. Sandora

FCDD- DAG-S/G. Steiger
FCDD- DAG-S/B. Vanamburg
6896 Mauchly St.
Aberdeen Proving Ground, MD 21005-5071

DEVCOM Army Research Laboratory
FCDD-RLD-CL/Tech Library
2800 Powder Mill Rd.
Adelphi, MD 20783-1138

U.S. Army Evaluation Center
Survivability Evaluation Directorate
TEEC-SV/RJ Spink
6617 Aberdeen Blvd., Bldg 2202, 2nd Floor
Aberdeen Proving Ground, MD 21005-5071

Defense Technical Information Center
ATTN: DTIC-O
8725 John J. Kingman Rd.
Fort Belvoir, VA 22060-6218

U.S. Army DEVCOM Ground Vehicle Systems Center
FCDD-GVR-VMT/D. Weyland
FCDD-GVR-VMT/R. Scherer
6501 E. 11 Mile Rd
Detroit Arsenal, MI 48397-5000

Office of the Director, Operational Test and Evaluation
OSD DOT&E
LFT&E/J. Ivancik
1700 Defense Pentagon 1D548
Washington, DC 20301